



RESEARCH PAPER

SQUINT promotes stem cell homeostasis and floral meristem termination in *Arabidopsis* through APETALA2 and CLAVATA signalling

Nathanaël Prunet^{1,2,*}, Patrice Morel¹, Priscilla Champelovier¹, Anne-Marie Thierry¹, Ioan Negrutiu¹, Thomas Jack² and Christophe Trehin^{1,†}

¹ Laboratoire de Reproduction et Développement des Plantes, Université de Lyon1, CNRS, INRA, ENS-Lyon, 46 allée d'Italie, F-69364 Lyon cedex 07, France

² Department of Biological Sciences, Class of 1978 Life Sciences Center, 78 North College Street, Dartmouth College, Hanover NH 03755, USA

* Present address: Department of Biology and Biological Engineering 156-29, California Institute of Technology, Pasadena, CA 91125, USA.

† To whom correspondence should be addressed. E-mail: ctrehin@ens-lyon.fr

Received 4 February 2015; Revised 20 July 2015; Accepted 27 July 2015

Editor: James Murray

Abstract

Plant meristems harbour stem cells, which allow for the continuous production of new organs. Here, an analysis of the role of SQUINT (SQN) in stem cell dynamics in *Arabidopsis* is reported. A close examination of *sqn* mutants reveals defects that are very similar to that of weak *clavata* (*clv*) mutants, both in the flower meristem (increased number of floral organs, occasional delay in stem cell termination) and in the shoot apical meristem (meristem and central zone enlargement, occasional fasciation). *sqn* has a very mild effect in a *clv* mutant background, suggesting that SQN and the CLV genes act in the same genetic pathway. Accordingly, a loss-of-function allele of SQN strongly rescues the meristem abortion phenotype of plants that overexpress CLV3. Altogether, these data suggest that SQN is necessary for proper CLV signalling. SQN was shown to be required for normal accumulation of various miRNAs, including miR172. One of the targets of miR172, APETALA2 (AP2), antagonizes CLV signalling. The *ap2-2* mutation strongly suppresses the meristem phenotypes of *sqn*, indicating that the effect of SQN on stem cell dynamics is largely, but not fully, mediated by the miR172/AP2 tandem. This study refines understanding of the intricate genetic networks that control both stem cell homeostasis and floral stem cell termination, two processes that are critical for the proper development and fertility of the plant.

Key words: APETALA2, CLAVATA signalling, floral meristem termination, flower development, SQUINT, stem cell homeostasis.

Introduction

Plant aerial growth results from the continuous production of new organs that derive from the shoot apical meristem (SAM), a dome of pluripotent cells, with a subpopulation of stem cells in the central zone (CZ). During vegetative growth, the SAM generates leaves, but, after the plant shifts to the

reproductive phase, it is converted to an inflorescence meristem (IM) and generates flower meristems (FMs) on its flanks. Each FM in turn produces the floral organs that form a flower. In *Arabidopsis thaliana*, stem cell maintenance in both the SAM and the FM relies on the homeodomain transcription

factor WUSCHEL (*WUS*; Laux *et al.*, 1996). The expression domain of *WUS* underlies the stem cells (Mayer *et al.*, 1998), but the *WUS* protein migrates to the stem cell niche, and this migration is necessary for stem cell maintenance (Yadav *et al.*, 2011). Mutation of *WUS* causes premature SAM arrest, but does not prevent initiation of new meristems, which subsequently abort (Laux *et al.*, 1996). Eventually, *wus* mutants produce some FMs, which similarly abort after producing a reduced number of floral organs.

In contrast, mutation in *CLAVATA1* (*CLV1*), *CLV2*, *CLV3*, or *CORYNE* (*CRN*) causes a phenotype opposite to that of *wus*, with an increase in both SAM and FM size (Clark *et al.*, 1993, 1995; Kayes and Clark, 1998; Muller *et al.*, 2008). *CLV1*–*CLV3* and *CRN* act in the same genetic pathway (Clark *et al.*, 1995; Kayes and Clark, 1998; Muller *et al.*, 2008). *CLV1* encodes a receptor-like kinase with extracellular leucine-rich repeats (LRRs; Clark *et al.*, 1997). *CLV2* and *CRN* resemble *CLV1*, but *CLV2* lacks the intracellular kinase domain (Jeong *et al.*, 1999), while *CRN* lacks the extracellular LRRs (Muller *et al.*, 2008). *CLV1* forms homomers while *CLV2* and *CRN* associate to generate a second receptor kinase complex (Muller *et al.*, 2008; Bleckmann and Simon, 2009). *CLV3* encodes a small, secreted protein that binds the *CLV1* ectodomain (Fletcher *et al.*, 1999; Rojo *et al.*, 2002; Lenhard and Laux, 2003; Kondo *et al.*, 2006; Ogawa *et al.*, 2008; Ohyama *et al.*, 2009). *CLV3* might also bind *CLV2*, and signal simultaneously through the *CLV1* and the *CLV2*–*CRN* receptor complexes (Muller *et al.*, 2008). *CLV3* also appears to signal in parallel through another receptor-like kinase, *RPK2* (Kinoshita *et al.*, 2010).

CLV signalling functions to restrict the number of cells that express *WUS*: the *WUS* expression domain expands in *clv* mutants, while *WUS* becomes undetectable when *CLV3* is overexpressed (Brand *et al.*, 2000; Schoof *et al.*, 2000). In turn, *WUS* directly activates *CLV3* expression in the stem cells (Yadav *et al.*, 2011). Stem cell homeostasis in both the SAM and FM therefore relies on a negative feedback loop between *WUS* and the *CLV* pathway, but other genes contribute to the fine-tuning of the stem cell population. One example is *APETALA2* (*AP2*), a transcriptional regulator that antagonizes *CLV* signalling (Wurschum *et al.*, 2006).

However, the growth patterns of the SAM and FM exhibit a major difference. The SAM is indeterminate, in that it continuously produces new structures throughout the life of the plant, while the FM is determinate and generates a precise number of floral organs before stem cells cease to be maintained. Floral determinacy (also known as FM termination) relies on a flower-specific negative feedback loop superimposed on that of *WUS/CLV*. Together with *LEAFY*, *WUS* activates *AGAMOUS* (*AG*) in the centre of the stage 3 flower (Lenhard *et al.*, 2001; Lohmann *et al.*, 2001) stages as described by Smyth *et al.* (1990). *AG*, in turn, represses *WUS* both directly and indirectly, and *WUS* mRNA becomes undetectable by stage 6, when carpel primordia arise (Mayer *et al.*, 1998; Sun *et al.*, 2009; Liu *et al.*, 2011). FM termination depends on proper *AG* expression in a subdomain at the centre of the flower, and numerous factors have been shown to be involved in *AG* transcriptional activation in this region (for reviews, see Prunet *et al.*, 2009; Ito, 2011). *clv1* mutants,

which exhibit delayed stem cell termination in the FM, specifically lack *AG* expression in this central subdomain (Clark *et al.*, 1993). This suggests that *CLV* signalling not only spatially restricts the population of stem cells within the FM, but also independently promotes their timely arrest through the activation of *AG*. Conversely, *AP2* is a direct repressor of *AG*, and increased *AP2* activity causes a loss of flower determinacy, associated with a defect of *AG* expression in the centre of the FM (Drews *et al.*, 1991; Jofuku *et al.*, 1994; Zhao *et al.*, 2007; Yant *et al.*, 2010).

Thus, defects in stem cell dynamics can result in two categories of phenotype. Defects in stem cell homeostasis cause changes in the size of the SAM and FM, and a variation in the number of floral organs within the four primary whorls. Conversely, a loss or delay of floral stem cell termination results in an indeterminacy phenotype, with extra whorls of floral organs forming within the flower. It is worth noting that both the *CLV* genes and *AP2* affect both stem cell homeostasis and termination, although to different extents.

The role of *SQUINT* (*SQN*) in FM termination was previously characterized (Prunet *et al.*, 2008). Mutation of *SQN* in a *crabs claw* (*crc*) mutant background causes a strong indeterminacy phenotype, with numerous supernumerary organs arising in between the carpels, a phenotype that results from a defect in *AG* expression in the centre of the FM (Prunet *et al.*, 2008). *SQN*, which was initially identified for its role in vegetative phase change, encodes the *Arabidopsis* orthologue of cyclophilin 40, a putative chaperone (Berardini *et al.*, 2001), and cannot regulate *AG* transcription directly. *SQN* was shown to be required for ARGONAUTE1 (*AGO1*) function and proper accumulation of miRNAs (Smith *et al.*, 2009; Earley *et al.*, 2010). *SQN* interacts with cytoplasmic Hsp90 proteins, which bind to *AGO1* and trigger the formation of the mature RISC complex, and the interaction between *SQN* and Hsp90 is required for *SQN* function (Iki *et al.*, 2010; Earley and Poethig, 2011). Accumulation of various miRNAs is reduced in *sqn* mutants (Smith *et al.*, 2009), including miR172, a negative regulator of *AP2* (Chen, 2004). This suggests a possible role for miR172 and *AP2* in the *sqn* indeterminacy phenotype.

In this study, a detailed phenotypic analysis of a *sqn* allelic series demonstrates that *sqn* mutants have meristem phenotypes similar to that of weak *clv* mutants. Moreover, a *sqn* loss-of-function mutation has a very mild effect in a *clv* mutant background, but strongly suppresses the meristem abortion phenotype associated with the overexpression of *CLV3*. It is also demonstrated that a mutation in miR172d causes defects similar to those observed in *sqn*, and that the *ap2-2* allele strongly, but not fully, suppresses the *sqn* meristem phenotypes. Taken together, the data suggest that *SQN* controls stem cell homeostasis and FM termination through the miR172/*AP2* tandem and the *CLV* signalling pathway.

Materials and methods

Plant growth and crosses

Plants were grown in soil, first for 3 weeks under short-day (10h light a day), 16 °C conditions, and then shifted to either long-day

(18h light d⁻¹), 20 °C or continuous day, 16 °C conditions. The strength of the meristem phenotypes of *sqn* and *clv* mutants varies with the growth conditions. This explains the discrepancies between different data sets presented herein. To eliminate this bias, each time mutants were compared, all genotypes were grown simultaneously in identical conditions. The *ap2-2*, *crc-1*, *clv1-2*, *clv1-4*, *clv1-6*, *clv3-2*, and *sqn-4* mutants are in the Landsberg *erecta* (*Ler*) ecotype. The *sqn-1*, *sqn-5*, *sqn-8*, *sqn-9*, *crc-8*, *miR172a-1*, and *miR172d-2* mutants are in Columbia-0 (Col0). The position of the mutations in the *sqn* and *miR172* alleles used in this study can be found in [Supplementary Table S1](#) available at *JXB* online. Analysis of the genetic interactions between *SQN* and the *CLV* genes was performed using *sqn-4*, to avoid segregating ecotype-specific traits, which may affect meristem size.

Construction of transgenic plants

The 35S::*CLV3* transgene was constructed by PCR amplification of *CLV3* cDNA using primers *CLV3*-forward and *CLV3*-reverse ([Supplementary Table S2](#) at *JXB* online). The PCR product was ligated into pCR8/GW/TOPO (Invitrogen), sequenced, and transferred into pK2GW7 ([Karimi et al., 2002](#)) using LR recombination. Transgenic plants were then generated as described by [Bechtold and Pelletier \(1998\)](#) and selected on Murashige and Skoog (MS) plates with kanamycin (50 µg l⁻¹).

Imaging and microscopy

Photographs of whole plants were taken using a Pentax K10D digital camera. Photographs of flowers, siliques, and shoot apices were taken with a DC300F digital camera mounted on a Leica MZFLIII stereomicroscope, and images were processed with the FW4000 software (Leica). FM4-64 membrane staining and green fluorescent protein (GFP) expression were monitored from homozygous plants using LSM-510 (Carl Zeiss) and AIRSi (Nikon) confocal microscopes, and images were processed with the LSM Image Browser (Zeiss), NIS-elements (Nikon), and Imaris software (Bitplane). Figures were composed with Adobe Photoshop CS6. To quantify the size of the SAM, the widest and narrowest diameters of the SAM of 10 wild-type and 10 *sqn-4* mutant plants at a depth of 5 µm and 15 µm under the meristem summit were measured and averaged. The size of the CZ was quantified with Imaris from confocal z-stacks of wild-type and *sqn-4* mutant SAMs homozygous for the *pCLV3::erGFP* reporter, using identical parameters for all plants for both live confocal imaging and Imaris.

Quantitative real-time RT-PCR

Total RNA was isolated from inflorescences of wild-type (*n*=5), 35S::*CLV3* (*n*=7), and *sqn-4* 35S::*CLV3* (*n*=8) plants using the Spectrum Plant Total RNA kit (Sigma) and treated with RQ1 DNase (Promega). A 1 µg aliquot of RNA was converted into cDNA using RevertAid M-MuLV-reverse transcriptase (Fermentas) and T11Vn primer. cDNAs were quantified using the DNA Engine opticon Real-Time PCR Detection System (Bio-Rad) with Platinum SYBR Green qPCR SuperMix UDG (Invitrogen). Primers *CLV3*-up and *CLV3*-down were used to amplify *CLV3* cDNAs; *WUS*-QPCR-F and *WUS*-QPCR-R to amplify *WUS* cDNAs; and For_1630 and Rev_1631 as well as For_1635 and Rev_1636 to amplify *SQN* cDNAs ([Supplementary Table S2](#) at *JXB* online). Normalization was performed using *GAPDH* (glyceraldehyde phosphate dehydrogenase) with primers *GAPDH*-forward and *GAPDH*-reverse, *TUBULIN4* with primers *TUB4*-forward and *TUB4*-reverse, and *ACTIN8* with primers *ACT8*-forward and *ACT8*-reverse. Calibration was performed using dilutions of a mix of cDNA from wild-type, 35S-*CLV3*, and *sqn-4* 35S::*CLV3* inflorescences, which explains why *CLV3* mRNA appears below the detection level in wild-type inflorescences.

Results

Loss of SQN function results in flower defects similar to that of weak *clv* mutants

Seven loss-of-function alleles of *SQN* have been described to date, all of which trigger a similar range of phenotypes, including defects in leaf initiation and shape, altered phyllotaxis, and increased carpel number ([Fig. 1A, B, E](#); [Berardini et al., 2001](#); [Prunet et al., 2008](#); [Smith et al., 2009](#)). The floral phenotype of the *sqn-1*, *sqn-4*, and *sqn-5* mutants, as well as two new T-DNA insertion alleles, *sqn-8* and *sqn-9*, was characterized in detail. These mutants are all in a Col0 background, except for *sqn-4*, which is in the *Ler* ecotype. They display floral phenotypes that are similar but differ in strength. *sqn-4* shows a significant increase in stamen and carpel number, but not in sepal and petal number ([Fig. 1E](#)). Conversely, *sqn-1* and *sqn-5* exhibit a significant increase in the number of all four types of floral organs ([Fig. 1E](#)). This increase in floral organ number is milder in the two outer whorls, and more severe in the two inner whorls. *sqn-9* has a milder phenotype, with an increase only in stamen number ([Fig. 1E](#)). *sqn-8* flowers do not differ from the wild type. In addition, stem cell termination is sometimes delayed in *sqn-1* and *sqn-5* flowers, with extra floral organs developing within the gynoecium ([Fig. 1C](#); [Table 1](#)), a phenotype that was not observed in *sqn-4*, *sqn-8*, and *sqn-9* when grown simultaneously for this experiment. However, the strength of the *sqn* phenotype varies depending on growth conditions, the general trend being that healthier, sturdier plants have a stronger phenotype. In different experiments, *sqn-4* plants actually showed an enhanced phenotype, with indeterminate flowers ([Fig. 1D, J](#)). When the Col0 *sqn* alleles are ordered into an allelic series based on the severity of the flower phenotype, *sqn-1* and *sqn-5*, which were inferred to be null alleles ([Smith et al., 2009](#)), are the strongest alleles, and *sqn-8* and *sqn-9* are the weakest alleles. With the notable exception of carpel number, the *Ler* allele *sqn-4* appears intermediate, in terms of both floral organ numbers and indeterminacy. Yet, *sqn-4* exhibits a stronger increase in carpel number than any other allele, including *sqn-1* and *sqn-5* ([Fig. 1E](#)), which may be an ecotype-specific effect, as the *ERECTA* gene was shown to control meristem size and *WUS* expression ([Mandel et al., 2014](#)). At the molecular level, *sqn-1*, *sqn-4*, and *sqn-5* have point mutations or T-DNA insertions that generate early stop codons in the *SQN* mRNA, while *sqn-8* and *sqn-9* have T-DNA insertions in the *SQN* promoter ([Supplementary Table S1](#) at *JXB* online). The *SQN* mRNA level appears reduced in *sqn-1*, *sqn-4*, and *sqn-8*, but, surprisingly, it is increased in *sqn-5* and *sqn-9* ([Supplementary Fig. S1](#)). However, the 3' end of the *SQN* mRNA is missing in *sqn-5* ([Supplementary Fig. S1](#)).

The flower phenotype of *sqn-1*, *sqn-4*, and *sqn-5* mutant plants is similar to that of weak *clv* mutants such as *clv1-2* and *clv1-6*, which show an increase in the number of all four types of floral organs, with a more pronounced increase in the inner whorls compared with the outer whorls ([Fig. 1A, E](#); [Clark et al., 1993](#)). The extra carpels that develop in the fourth whorl of both *sqn* and *clv* mutant flowers sometimes arise in the upper half of the gynoecium, and modify its morphology,

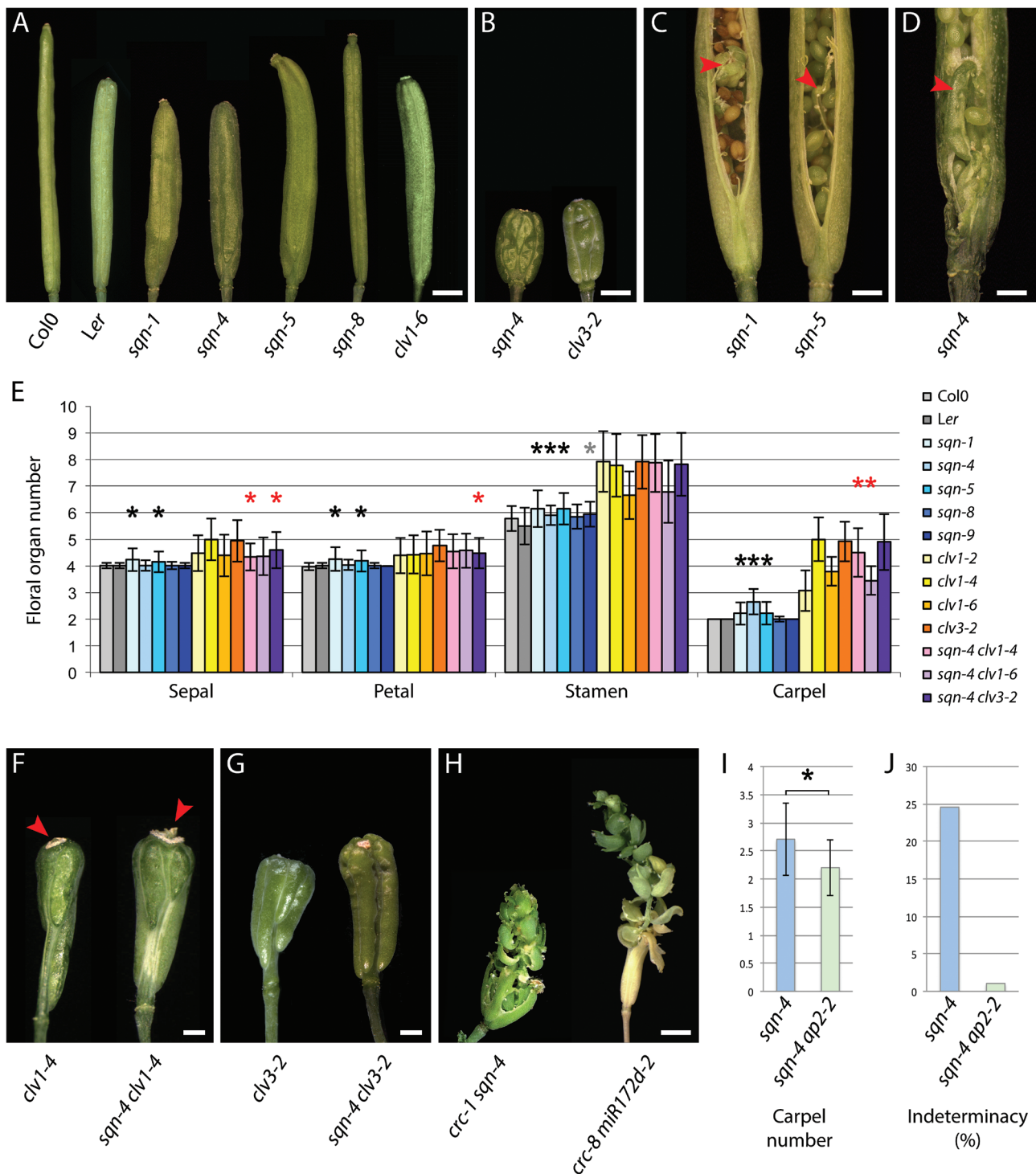


Fig. 1. Floral phenotype of various mutant combinations. (A) From left to right, representative siliques of wild-type Col0 and *Ler*, *sqn-1*, *sqn-4*, *sqn-5*, *sqn-8*, and *clv1-6* plants. (B) Left, silique of an *sqn-4* plant showing an extreme increase in carpel number; right, representative silique of a *clv3-2* plant. (C) Opened siliques of *sqn-1* (left) and *sqn-5* (right) plants grown in long-day conditions, showing extra carpels (red arrowheads) developing inside the gynoeceum. (D) Opened silique of an *sqn-4* plant grown in continuous-day conditions, showing extra carpels (red arrowheads) developing inside the gynoeceum. (E) Floral organ numbers of wild-type (shades of grey), *sqn* single mutant (shades of blue), *clv* single mutant (shades of yellow), and *sqn-4 clv* double mutant (shades of purple) plants; a detailed key for the genotypes is on the right of the graph. Black and grey asterisks indicate significant differences from the wild type (Student's *t*-test, $P < 0.01$ and $P < 0.05$, respectively). Red asterisks indicate significant differences from the corresponding single *clv* mutant (Student's *t*-test, $P < 0.01$). (F) Representative siliques of the *clv1-4* (left) and *sqn-4 clv1-4* (right) mutants. Red arrowheads point at the FM proliferating through the carpels, which are not fully fused at their tip. (G) Representative siliques of the *clv3-2* (left) and *sqn-4 clv3-2* (right) mutants. (H) Representative siliques of the *crc-1 sqn-4* (left) and *crc-8 mir172d-2* (right) mutants, showing a strong loss of FM determinacy. (I, J) Carpel number (I) and indeterminacy rate (J) of *sqn-4* and *sqn-4 ap2-2* mutants. The asterisk in I indicates a significant difference (Student's *t*-test, $P < 0.0001$). Scale bars=1 mm in A, B, and H, and 500 μ m in C, D, F, and G.

making it club-shaped (Supplementary Fig. S2 at *JXB* online; Clark *et al.*, 1993; Prunet *et al.*, 2008). Additionally, the gynoecium of some *sqn-4* flowers consists of up to eight carpels, similar to that of strong *clv* mutants such as *clv1-4* and *clv3-2* (Fig. 1B). Finally, *sqn* flowers have defects in stem cell termination, although to a lesser extent than *clv* flowers (Table 1; Clark *et al.*, 1993, 1995; Kayes and Clark, 1998). Mutations in *SQN* and *CLV1* also cause similar defects in other genetic backgrounds. For instance, both *sqn-4 ag-6* and *sqn-4 ag-4* double mutant flowers are often fasciated: they appear much larger and contain many more floral organs than *ag-6* and *ag-4* single mutant flowers (Fig. 2, compare A and B, C and D), a phenotype also seen in *clv1 ag* double mutants (Clark *et al.*, 1993).

sqn-4 exhibits enlarged inflorescence meristems and central zones

The expression of *SQN* is not restricted to flowers: *SQN* is broadly expressed throughout the plant (Prunet *et al.*, 2008). Experiments were carried out to determine whether *sqn* also exhibits *clv*-like defects in the SAM. Inflorescences of *sqn-4*

mutant plants appear larger than those of wild-type plants (Fig. 3A, B), like those of *clv* mutants (Clark *et al.*, 1993, 1995; Kayes and Clark, 1998). Live confocal imaging was used to assess the size of the SAM in wild-type and *sqn-4* plants. The SAM of *sqn-4* plants is significantly larger than that of the wild type, with a 55–92% increase in width, depending on the depth where the measurement is taken within the meristem (Fig. 3K). Also, the SAM of *sqn-4* plants is sometimes fasciated (Fig. 3I, J; Supplementary Fig. S3 at *JXB* online), a phenotype that is typical of *clv* mutants and usually results in massively enlarged and flattened stems (Clark *et al.*, 1993, 1995; Kayes and Clark, 1998). Interestingly, despite this occasional fasciation of the SAM, *sqn-4* plants rarely exhibit flat stems. This may be due to the fact that branching of the meristem often follows fasciation in *sqn-4* (Fig. 2J; Supplementary Fig. S3), thus preventing the formation of large, fasciated stems.

The size of the CZ was also assessed in wild-type and *sqn-4* inflorescences, using the *pCLV3::erGFP* reporter line (Reddy and Meyerowitz, 2005). The CZ appears both wider and higher in *sqn-4* mutants compared with the wild type (Fig. 3C, D; Supplementary Fig. S4A, B at *JXB* online). In fasciated *sqn-4*

Table 1. Indeterminacy phenotype of *sqn*, *clv*, and *sqn-4 clv* mutants

	Indeterminate flowers (%)	<i>n</i>	Flowers with a fifth whorl (%)	Flowers with a sixth whorl (%)	Flowers with an outgrowing FM (%)	<i>n</i>
Col0	0	100	–	–	–	–
Ler	0	100	–	–	–	–
<i>sqn-1</i>	20	100	–	–	–	–
<i>sqn-4</i>	0	100	0	0	0	100
<i>sqn-5</i>	32	100	–	–	–	–
<i>sqn-8</i>	0	100	–	–	–	–
<i>sqn-9</i>	0	100	–	–	–	–
<i>clv1-2</i>	96.2	80	–	–	–	–
<i>clv1-4</i>	100	100	100	85.5	58.2	110
<i>clv1-6</i>	89	100	35	0	0	60
<i>clv3-2</i>	100	100	93.9	70.5	55	110
<i>sqn-4 clv1-4</i>	100	100	99.5	94.7	71.6	210
<i>sqn-4 clv1-6</i>	99	100	95	30	0	60
<i>sqn-4 clv3-2</i>	100	100	100	93.4	53.4	140

This table presents two independent data sets: an overall quantification of the indeterminacy phenotype of all mutants (left columns), and a more detailed analysis of this indeterminacy phenotype for some of these mutants (right columns). *n*, number of flowers counted.

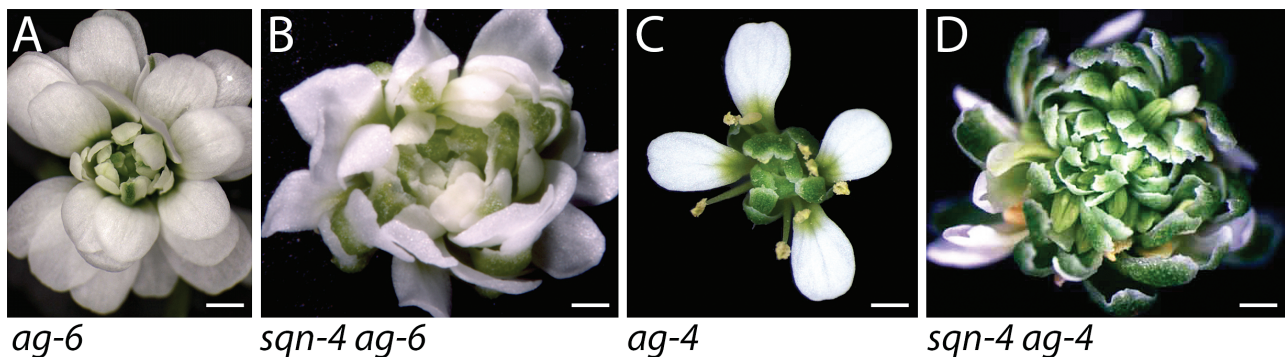


Fig. 2. *sqn-4* causes fasciation in *ag* mutant flowers. (A) *ag-6* flower. (B) *sqn-4 ag-6* flower displaying many more floral organs than an *ag-6* flower. (C) *ag-4* flower. (D) Fasciated *sqn-4 ag-4* flower. Scale bars=500 μ m.

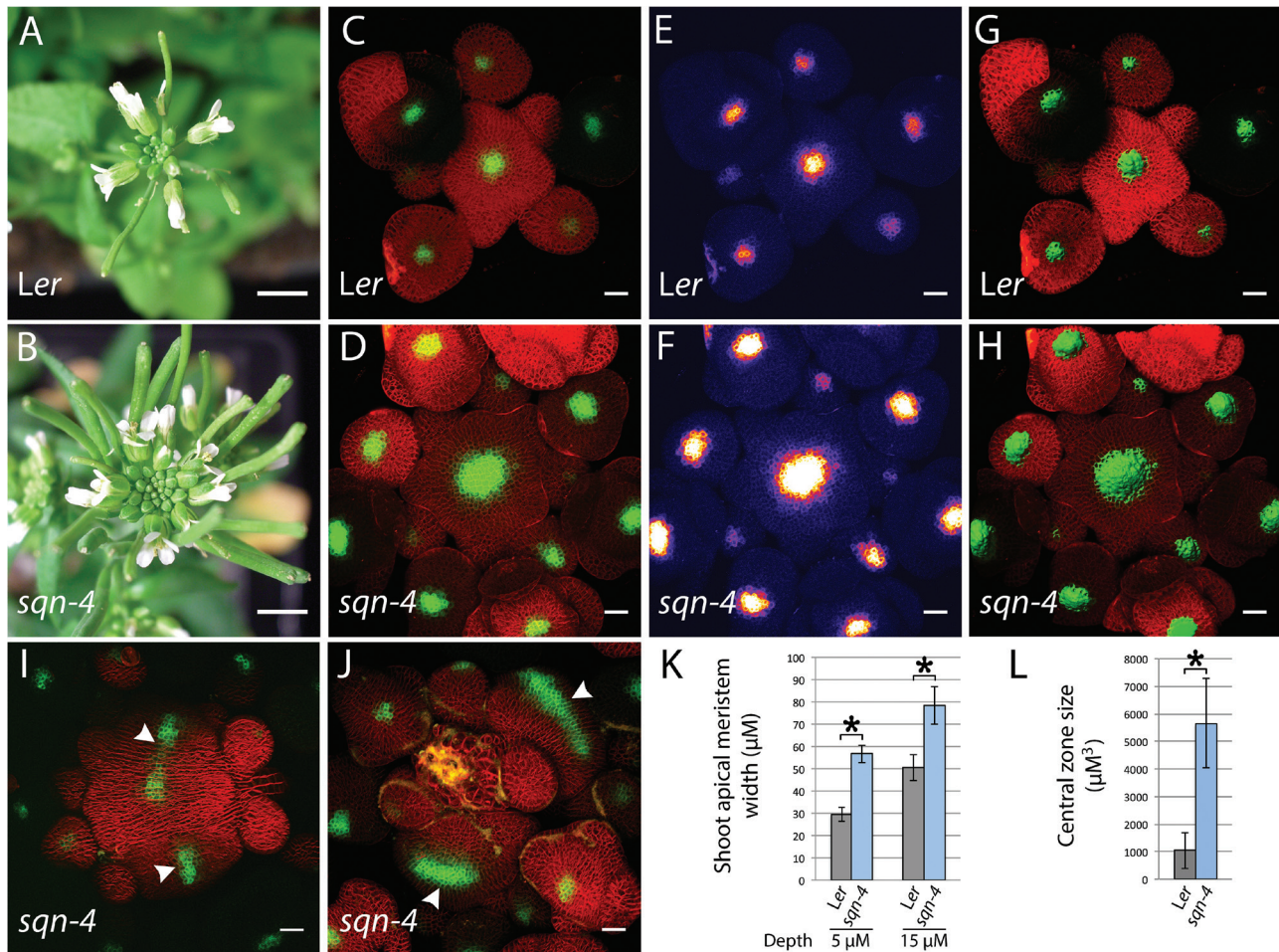


Fig. 3. *sqn-4* causes an increase in inflorescence meristem and central zone size. (A, B) Apical view of wild-type Ler (A) and *sqn-4* (B) inflorescences. (C–H) Apical view of wild-type Ler (C, E and G) and *sqn-4* (D, F and H) IMs expressing a *pCLV3::erGFP* reporter. (C–F) Maximum intensity projection of confocal z-stacks; (G, H) 3D reconstructions of the same confocal stacks obtained with Imaris. (C, D) Green, GFP; red, FM4-64-stained plasma membranes. (E, F) The intensity of the GFP signal as indicated by a fire colour code: the brighter the colour, the stronger the signal. (G, H) Green, volumes within the inflorescence and flower meristems with GFP expression, as detected using Imaris; red, FM4-64-stained plasma membranes. (I, J) Fasciated *sqn-4* inflorescences expressing *pCLV3::erGFP*. Arrowheads point at the CZ(s) of the IMs. In (I), the elongated CZ has split into two distinct domains. In (J), the initial IM has split into two meristems. (K, L) Width of the SAM (K) and size of the CZ (L) of wild-type Ler (grey) and *sqn-4* (light blue) plants. (K) The maximum and minimum width of 10 SAMs of each genotype was measured at a depth of 5 μm (left histograms) and 15 μm (right histograms), and averaged. (L) Mean CZ volume, as measured with Imaris from confocal z-stacks. Error bars represent the SD. Black asterisks indicate significant differences (Student's *t*-test, $P < 0.0001$ in L and $P < 0.001$ in K). Scale bars = 5 mm in A, B, and 10 μm in C–J.

meristems, the CZ is linear, rather than circular (Fig. 3I, J), and often separates into two distinct domains (Fig. 3I), an event that probably precedes the branching of the meristem. Confocal z-stacks were processed with Imaris to quantify the volume of cells expressing *pCLV3::erGFP* within the SAM (Fig. 3G, H; Supplementary Fig. S4). The volume of the CZ is significantly increased in *sqn-4* compared with the wild type (Fig. 3L). The *CLV3* expression domain also appears enlarged in *sqn-4* FMs (Fig. 3C, D), and, based on the level of GFP fluorescence, the *CLV3* expression level is higher in *sqn-4* flowers than in the wild type (Fig. 3E, F). Overall, this SAM and CZ enlargement phenotype reinforces the similarity between the *sqn* and *clv* mutants.

Genetic interactions suggest that SQN and the CLV genes act in the same pathway

The similarities between *sqn* and weak *clv* mutants prompted an investigation of the genetic interactions between *SQN* and

the *CLV* genes. To this end, *sqn-4* was crossed with one weak (*clv1-6*) and two strong (*clv1-4* and *clv3-2*) *clv* alleles. *clv1-6* results in a loss of CLV signalling through the CLV1 receptor complex only. In contrast, *clv1-4* is a dominant-negative allele that is postulated to affect CLV signalling through both the CLV1 and CLV2–CRN receptor complexes, due to cross-talk between these complexes (Dievart et al., 2003; Muller et al., 2008). Signalling through both receptor complexes is similarly affected in *clv3-2*, due to the lack of functional ligand. CLV signalling is thus only partly defective in *clv1-6*, while it is strongly or fully impaired in *clv1-4* and *clv3-2*.

Both *clv1-4* and *clv3-2* have enlarged SAMs and FMs, with an increase in primary floral organ number, and delayed stem cell termination in the FM (Fig. 1E–G; Table 1; Clark et al., 1993, 1995). After one or two extra whorls have been produced, the FM usually overproliferates, becomes irregularly shaped, and sometimes grows through the apex of the gynoecium, where carpels are often imperfectly fused (Fig. 1F).

sqn-4 clv1-4 and *sqn-4 clv3-2* double mutants are morphologically indistinguishable from *clv1-4* and *clv3-2* single mutants, respectively (Fig. 1F, G), thus the double mutants had to be identified via PCR-based genotyping. However, some statistical differences were observed between the *sqn-4 clv* double mutants and the corresponding *clv* single mutants. Surprisingly, the number of sepals and carpels is slightly, but significantly reduced in *sqn-4 clv1-4* compared with *clv1-4*, and the number of sepals and petals is similarly reduced in *sqn-4 clv3-2* compared with *clv3-2* (Fig. 1E). However, the main difference between *sqn-4 clv* double mutants and the corresponding *clv* single mutants lies in the strength of the indeterminacy phenotype: the loss of stem cell termination in *clv1-4* and *clv3-2* flowers is statistically increased by the *sqn-4* mutation. Most *clv1-4*, *clv3-2*, *sqn-4 clv1-4*, and *sqn-4 clv3-2* flowers are indeterminate (Table 1). Nevertheless, the proportion of *sqn-4 clv1-4* flowers either producing six whorls (i.e. two extra whorls inside the gynoecium) or exhibiting an overgrowth of the FM through the primary carpels is higher than that of *clv1-4* flowers (Table 1). Similarly, the proportion of *sqn-4 clv3-2* flowers producing at least five or six whorls is higher than that of *clv3-2* flowers (Table 1). Even though *sqn* subtly alters the *clv* phenotypes, the phenotype of *sqn-4 clv1-4* and *sqn-4 clv3-2* double mutant flowers always remains within the range of phenotypes caused by the *clv1-4* and *clv3-2* mutations alone, suggesting that *SQN* controls stem cell dynamics largely through the same pathway as the *CLV* genes.

The *sqn-4* mutation has little effect on the primary floral organ number of the weak *clv1-6* mutant (Fig. 1E), but it strongly modifies its indeterminacy phenotype. While only one-third of *clv1-6* flowers exhibits a fifth whorl and none produces a sixth whorl, almost every *sqn-4 clv1-6* flower produces a fifth whorl, and nearly one-third develops a sixth whorl (Table 1). Thus, *sqn-4* enhances the loss of the FM indeterminacy phenotype of *clv1-6*, making it more similar to strong *clv* alleles, further supporting the idea that *SQN* and the *CLV* genes control stem cell dynamics through the same genetic pathway.

SQN is required for constitutive CLV signalling

In an effort to determine whether the *sqn* mutation affects constitutive CLV signalling, which normally results in a *wus*-like phenotype, with a premature arrest of both SAM and FMs (Brand *et al.*, 2000), wild-type and *sqn-4* plants were transformed with a *35S::CLV3* construct. All *35S::CLV3* plants that we analysed ($n=14$) initiated, but failed to maintain SAMs, resulting in a bushy and highly branched phenotype similar to that of *wus* mutants (Fig. 4B, C). Some *35S::CLV3* plants bolted (Fig. 4C), but their IMs aborted after producing a few terminal leaves or flowers (Fig. 4C, E, F). Conversely, nine out of 10 *sqn-4 35S::CLV3* plants maintained their IMs (Fig. 4D, G–J), although the inflorescences were sometimes smaller than those of wild-type plants (Fig. 4G, K). A similar effect of the *sqn-4* mutation was observed on flower development in plants overexpressing *CLV3*. Like *wus* mutants, *35S::CLV3* flowers exhibited a reduced number of stamens and no carpels, and, after

senescence, no floral organs remained on the peduncle (Supplementary Fig. S5A at JXB online). Conversely, *sqn-4 35S::CLV3* flowers usually produced a normal number of stamens and either a normal gynoecium (Fig. 4D, J) or a carpelloid filament, which remained on the peduncle after senescence of the flower (Fig. 4H, J; Supplementary Fig. S5B). Quantitative reverse transcription PCR (RT-PCR) analyses confirmed that these differences were not due to co-suppression of *CLV3* in the *sqn-4* mutant background, as *35S::CLV3* and *sqn-4 35S::CLV3* plants expressed *CLV3* at similar, very high levels (Fig. 4A). Moreover, quantification of *WUS* expression showed that overexpression of *CLV3* was sufficient to reduce *WUS* expression strongly in an otherwise wild-type background, but failed to down-regulate *WUS* in *sqn-4* consistently (Fig. 4A). Thus, the *sqn-4* mutation strongly rescues both the IM and the FM phenotype of *35S::CLV3* plants, suggesting that *SQN* is required for constitutive CLV signalling.

ap2-2 strongly suppresses the meristem phenotypes of sqn

SQN is required for the proper accumulation of several miRNAs (Smith *et al.*, 2009). The level of the miRNA miR172, in particular, is reduced by 40% in *sqn-1* compared with the wild type. The targets of miR172 include *AP2*, which antagonizes both *AG* and the CLV pathway (Drews *et al.*, 1991; Jofuku *et al.*, 1994; Chen, 2004; Wurschum *et al.*, 2006; Zhao *et al.*, 2007). Thus, down-regulation of miR172 in a *sqn* mutant background could account for the meristem phenotypes described above. The potential role of miR172 and *AP2* in the floral phenotype of *sqn* mutants was therefore investigated.

Unlike *sqn* mutants, neither the *miR172a-1* and *miR172d-2* single mutants nor the *miR172a-1 miR172d-2* double mutant exhibit extra carpels in the fourth whorl or extra organs within the gynoecium, but *miR172d-1* single mutant flowers were recently reported occasionally to have three carpels (Yumul *et al.*, 2013). Similarly, the *miR172a-1* mutation has no effect in a *crc-8* mutant background. However, 9.6% of *crc-8 miR172d-2* double mutant flowers ($n=100$) are indeterminate, and occasionally exhibit a strong loss of FM termination, with numerous stamens and carpels borne on a stem growing outside the primary gynoecium, a phenotype also seen in *crc-1 sqn-4* flowers (Fig. 1H; Prunet *et al.*, 2008). This phenotype is statistically stronger in the *crc-8 miR172a-1 miR172d-2* triple mutant, with 17.7% of flowers being indeterminate ($n=100$). Despite this similarity, the indeterminacy phenotype of *crc-8 miR172d-2* and *crc-8 miR172a-1 miR172d-2* plants is statistically weaker than that of *crc-1 sqn-4*, in which 100% of flowers ($n=100$) are indeterminate. Nonetheless, the similar effect of the *sqn-4* and *miR172d-2* mutations in a *crc* mutant background, together with the increased carpel number in both *sqn-4* and *miR172d-1*, suggests that the down-regulation of miR172 may be at least partly responsible for the meristem phenotype of the *sqn* mutants.

The role of one of the targets of miR172, *AP2*, was thus investigated in this phenotype. The *ap2-2* allele strongly suppresses both the increase in carpel number and the

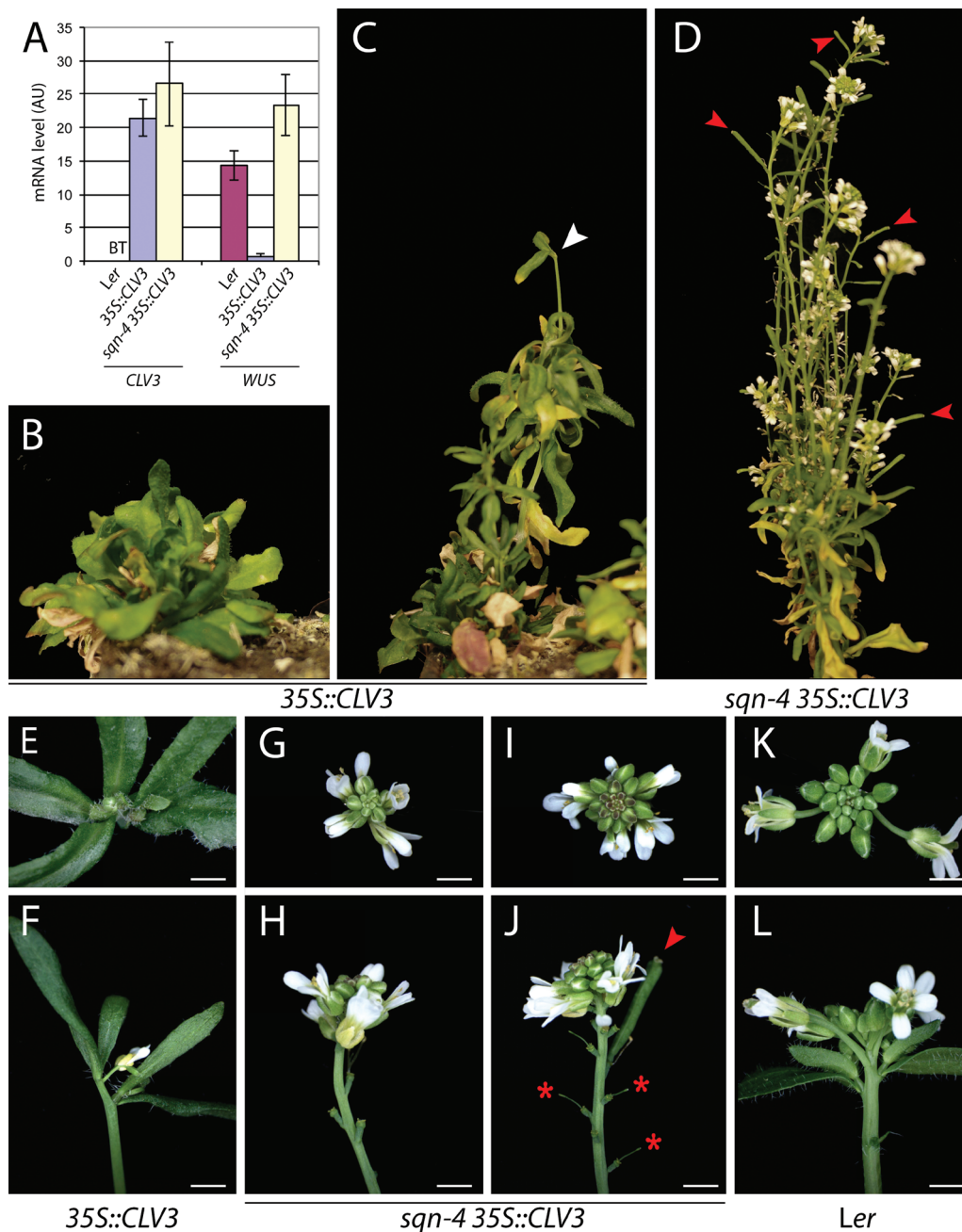


Fig. 4. The *sqn-4* mutation rescues the 35S::CLV3 phenotype. (A) From left to right: CLV3 mRNA levels in wild-type, 35S::CLV3, and *sqn-4* 35S::CLV3 inflorescences, and WUS mRNA levels in wild-type, 35S::CLV3, and *sqn-4* 35S::CLV3 inflorescences. CLV3 mRNA was below the detection threshold (BT) in the wild type. The CLV3 mRNA level does not significantly differ between 35S::CLV3 and *sqn-4* 35S::CLV3 inflorescences. The WUS mRNA level significantly differs between 35S::CLV3 and *sqn-4* 35S::CLV3 inflorescences (Student's *t*-test, $P < 0.01$), but not between wild-type and *sqn-4* 35S::CLV3 inflorescences. Error bars represent The SEM. AU, arbitrary units. (B–D) Overall morphology of 35S::CLV3 (B, C) and *sqn-4* 35S::CLV3 plants (D). (B) 35S::CLV3 plant that failed to bolt; regular initiation and subsequent abortion of SAMs confers on the rosette a bushy aspect. (C) 35S::CLV3 plant that eventually bolts; the IM aborted (white arrowhead) after producing two terminal leaves. (D) *sqn-4* 35S::CLV3 plant that maintained several IMs, which produced normal siliques (red arrowheads) after bolting. (E–L) Apical view (E, G, I, K) and side view (F, H, J, L) of inflorescences of 35S::CLV3 (E, F), *sqn-4* 35S::CLV3 (G, J), and wild-type plants (K, L). Red asterisks indicate carpelloid filaments; the red arrowhead points to a normal silique. Scale bars=1500 μ m.

indeterminacy phenotype of *sqn-4* mutant flowers (Fig. 11, J). However, this suppression is not complete, as some *sqn-4* *ap2-2* flowers exhibit three or four carpels, and sometimes a fifth whorl, a phenotype never observed in *ap2-2*. Altogether, the data suggest that the meristem phenotypes of *sqn* mutants are largely, but not entirely, due to a decrease in miR172 levels and a subsequent increase in AP2 levels.

Discussion

SQN controls stem cell homeostasis by modulating CLV signalling downstream of CLV3

SQN was initially described for its role in promoting juvenile-to-adult phase change and FM termination (Berardini *et al.*, 2001; Prunet *et al.*, 2008). Here, it is shown that *SQN* also

controls stem cell homeostasis in both the SAM and FM. Several pieces of evidence suggest that *SQN* acts through the same genetic pathway as the *CLV* genes. First, a detailed phenotypic analysis reveals that the *sqn* and *clv* mutants have similar phenotypes, both in the SAM, which appears enlarged and occasionally fasciated (Fig. 3), and in the FM, which produces more floral organs than the wild type, and, sometimes, extra whorls within the gynoecium (Fig. 1; Table 1; Clark *et al.*, 1993, 1995; Kayes and Clark, 1998). In both *sqn* and *clv* mutants, these meristem phenotypes are associated with an increase in the stem cell population, as well as a prolonged maintenance of the stem cells in the flower, as indicated by the monitoring of the *CLV3* stem cell marker (Fig. 3; Fletcher *et al.*, 1999; Prunet *et al.*, 2008). Mutations in *SQN* and the *CLV* genes also result in similar defects in an *ag* mutant background, with the formation of fasciated flowers (Fig. 2; Clark *et al.*, 1993). Secondly, an *sqn* loss-of-function mutation enhances the phenotype of a weak *clv* allele, but has only a mild effect in a strong *clv* mutant background. Despite some statistical differences, *sqn clv* double mutants are morphologically indistinguishable from *clv* single mutants. This is in stark contrast to what is observed when other mutants that affect meristem size, such as *ultrapetalal* (*ult1*), are crossed to the *clv* mutants. Mutations in *ULT1* and *SQN* cause very similar defects, including an increase in SAM size and floral organ number, a delay in FM termination, and a reduction of *AG* expression in the centre of the FM (Figs 1, 3; Fletcher, 2001; Carles *et al.*, 2004; Prunet *et al.*, 2008); yet, in contrast to *sqn clv*, the phenotype of *ult1 clv* double mutants is dramatically stronger than that of *clv* single mutants (Fletcher, 2001). Thirdly, the *sqn* mutation strongly prevents the repression of *WUS* and the associated *wus*-like phenotype normally caused by the overexpression of *CLV3*, showing that *SQN* is required for constitutive *CLV* signalling, and acts downstream of *CLV3*. Fourthly, *WUS* is epistatic to both *SQN* and the *CLV* genes (Schoof *et al.*, 2000; Prunet *et al.*, 2008). Finally, SHEPHERD (SHD), another chaperone that belongs to the Hsp90 family, was suggested to control stem cell homeostasis through the *CLV* pathway (Ishiguro *et al.*, 2002). Like *sqn*, a mutation in *SHD* causes a *clv*-like phenotype, has little effect in a *clv* mutant background, and suppresses the *wus*-like phenotype associated with the overexpression of *CLV3*. Altogether, these data indicate that *SQN* and the *CLV* genes largely act in the same genetic pathway to restrict *WUS* expression and control stem cell homeostasis. Based on this, *SQN* probably functions to promote *CLV* signalling downstream of *CLV3* (Fig. 5).

The effect of *SQN* on *CLV* signalling appears sufficient to explain the increase in floral organ number and meristem size in the *sqn* mutants. It may also contribute to the delay in stem cell termination in *sqn* mutant flowers. The indeterminacy phenotype of *sqn* mutants was previously linked to a decrease in *AG* expression in the centre of the flower, but it was argued that this down-regulation was probably indirect, given the putative chaperone function of *SQN* (Prunet *et al.*, 2008). A similar defect in *AG* expression has been described in the centre of *clv* mutant flowers (Clark *et al.*, 1993), making the *CLV* signalling pathway one likely intermediate between *SQN* and *AG* (Fig. 5). However, while the *sqn* mutation has

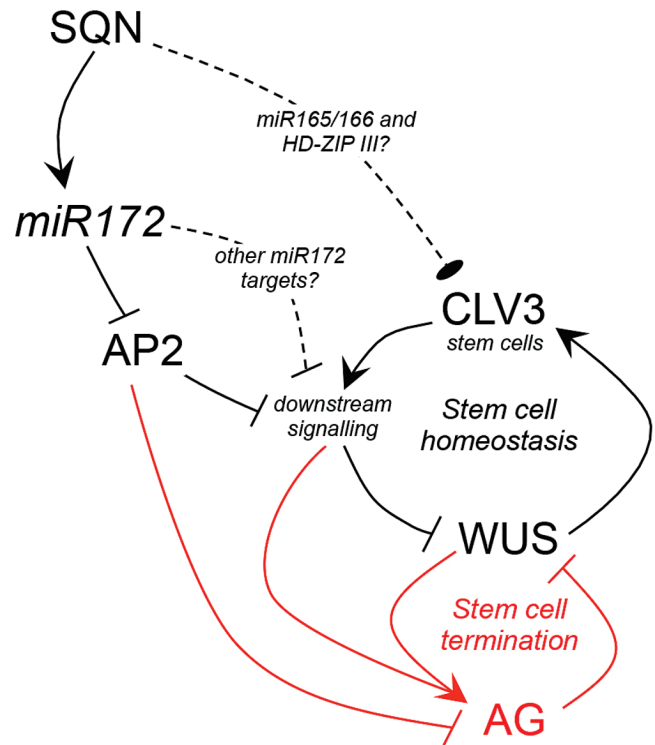


Fig. 5. Model for an AP2/*CLV*-mediated control of stem cell dynamics by *SQN* in the SAM and FM. In both the SAM and FM, stem cell homeostasis relies on a negative feedback loop between the stem cell-promoting gene *WUS* and the *CLV* signalling pathway. In the FM, an additional negative feedback loop between the flower-specific transcription factor *AG* and *WUS* ensures the timely arrest of stem cell maintenance. In both the SAM and the FM, *SQN* contributes to stem cell homeostasis mostly through miR172/AP2 and *CLV* signalling. *SQN* allows for proper accumulation of miR172, which in turn dampens AP2 levels. This results in a positive effect of *SQN* on *CLV* signalling, downstream of *CLV3*, as AP2 antagonizes *CLV* signalling. Other targets of miR172, as well as other miRNAs and their targets, such as miR165/166 and *HD-ZIP III* genes, might contribute in a minor way to the effect of *SQN* on stem cell homeostasis. In the FM, *SQN* also promotes stem cell termination. This effect is also mostly mediated by the miR172/AP2 tandem, which controls the expression of *AG*. The *CLV* signalling pathway contributes to the proper activation of *AG* in the centre of the flower. However, in contrast to the effect of *SQN* on stem cell homeostasis, the effect of *SQN* on stem cell termination is not entirely mediated by *CLV* signalling. *SQN* reduces the level of AP2, which represses *AG* expression indirectly, through its effect on *CLV* signalling, but also directly. Black indicates events that take place in both the SAM and FM; red indicates flower-specific events. Arrows indicate activations, and blunt-ended lines repressions. The oval-ended line indicates the complex influence *HD-ZIP III* genes have on the stem cells. Dashed arrows indicate hypothetical interactions that might have a minor effect on stem cell dynamics but have not been tested experimentally.

little effect on floral organ number in *clv* mutant flowers, it significantly enhances the indeterminacy phenotype of *clv* mutants (Table 1). This suggests that modulation of *CLV* signalling by *SQN* may fully account for the role of *SQN* in stem cell homeostasis, but not in floral meristem termination.

The miR172/AP2 tandem mediates an important part of the effects of SQN on stem cell dynamics

How does *SQN*, a putative chaperone, influence *CLV* signalling? While the Hsp90 protein SHD was proposed to

assist the folding of members of the CLV pathway (Ishiguro *et al.*, 2002), available data suggest that SQN is unlikely to function via the same molecular mechanism. First, SQN is cytoplasmic, while SHD is localized in the endoplasmic reticulum (Ishiguro *et al.*, 2002; Prunet *et al.*, 2008). Secondly, no interaction between SQN and members of the CLV pathway was identified through yeast two-hybrid experiments (data not shown). Thirdly, both SQN and Hsp90 proteins were shown to promote AGO1 function (Smith *et al.*, 2009; Earley *et al.*, 2010; Iki *et al.*, 2010). While no direct interaction between SQN and AGO1 has been shown, SQN binds to cytoplasmic Hsp90 proteins, which bind to AGO1, and the interaction between SQN and Hsp90 is required for SQN function (Smith *et al.*, 2009; Earley *et al.*, 2010; Earley and Poethig, 2011). Reduced AGO1 function in *sqn* causes a reduction in the accumulation of various miRNAs, which can potentially explain most of the phenotypes of the *sqn* mutant (Smith *et al.*, 2009). Down-regulation of miR156 is critical for the precocious vegetative phase-change phenotype of the *sqn* mutant, and may also explain its aberrant phyllotaxis (Smith *et al.*, 2009), but it is unlikely to account for the *sqn* meristem phenotypes. The accumulation of miR172, which targets *AP2* (Aukerman and Sakai, 2003; Chen, 2004), is also strongly reduced in *sqn* (Smith *et al.*, 2009). Since *AP2* both represses *AG* and antagonizes CLV signalling (Drews *et al.*, 1991; Jofuku *et al.*, 1994; Wurschum *et al.*, 2006), it seemed likely that reduced levels of miR172, and the resulting increase in *AP2* protein abundance, cause, or at least contribute to, the meristem phenotypes observed in *sqn* mutants. Indeed, the fact that a mutation in miR172d triggers an increase in carpel number (Yumul *et al.*, 2013), as well as an indeterminacy phenotype similar to that of *sqn* in a *cre* mutant background (Fig. 1H), supports this hypothesis. Accordingly, the strong *ap2-2* allele strongly suppresses both the increase in carpel number and the floral indeterminacy phenotype of *sqn* mutants, suggesting that the miR172/*AP2* tandem mediates an important part of the effect of SQN on both stem cell homeostasis and FM termination (Fig. 5).

The involvement of *AP2* downstream of SQN probably explains why a mutation in SQN has little effect on floral organ number in *clv* mutants, but enhances flower indeterminacy. *AP2* influences stem cell homeostasis by antagonizing CLV signalling (Wurschum *et al.*, 2006; Zhao *et al.*, 2007), but potentially affects FM termination through two different pathways: one independent of, and one dependent on, CLV signalling, both of which converge on *AG* (Fig. 5). *AP2* represses *AG* directly, but also indirectly, through its effect on the CLV pathway, which promotes *AG* expression in the centre of the flower (Drews *et al.*, 1991; Clark *et al.*, 1993; Jofuku *et al.*, 1994).

It is also worth noting that when Wurschum *et al.* (2006) proposed that *AP2* affects CLV signalling, they could not rule out the alternative possibility that *AP2* regulates *WUS* antagonistically, but independently of the CLV pathway. By linking SQN to the CLV pathway via *AP2*, the present data confirm that *AP2* affects CLV signalling downstream of *CLV3*.

Other factors may contribute to the effect of SQN on stem cell homeostasis

The *ap2-2* mutation does not completely suppress the increase in carpel number and floral indeterminacy of *sqn* mutants, suggesting that part of the effect of SQN on stem cell homeostasis and termination is independent of *AP2*. In addition to *AP2*, miR172 targets five other genes (Park *et al.*, 2002; Aukerman and Sakai, 2003; Schmid *et al.*, 2003; Chen, 2004). These six target genes function partially redundantly to control flowering time (Yant *et al.*, 2010). This redundancy may similarly explain why the *ap2-2* mutation fails to suppress the phenotype of *sqn* fully, as some of the five other targets of miR172 may compensate for the loss of *AP2* and repress *AG* and CLV signalling in these mutants (Fig. 5).

It is also possible that miRNAs other than miR172 are involved (Fig. 5). For instance, miR165/166 and their HD-ZIPIII targets have been shown to affect stem cell homeostasis and termination (Prigge *et al.*, 2005; Williams *et al.*, 2005; Ji *et al.*, 2011). The accumulation of miR165 is reduced by 10% in *sqn-1* compared with the wild type (Smith *et al.*, 2009), but the levels of miR166 have not yet been investigated. In any case, it is difficult to foresee the potential effects of decreased levels of miR165/166 on stem cell dynamics in the SAM and FM, as the influence of HD-ZIPIII genes on stem cell homeostasis is complex. Gain-of-function, miR165/166-resistant alleles of *PHABULOSA* (*PHB*) and *PHAVOLUTA* (*PHV*) cause flower indeterminacy in some mutant backgrounds, but so does overexpression of miR165/166 (Ji *et al.*, 2011). Increased levels of miR166 in the *jabbal-D* mutant, and the subsequent decrease in *PHB*, *PHV*, and *CORONA* (*CNA*) expression, result in SAM fasciation but also in a reduction in carpel number (Williams *et al.*, 2005). In contrast, the simultaneous loss of function of *PHB*, *PHV*, and *CNA* triggers an increase in carpel number and occasional indeterminacy (Prigge *et al.*, 2005). The somewhat contradictory effect of HD-ZIPIII genes on stem cells suggests that reduced levels of miR165/166 may contribute to the *AP2*-independent meristem phenotypes of *sqn* (Fig. 5). Interestingly, this contradictory effect might also explain why the number of some floral organs is slightly reduced in some *sqn clv* double mutants compared with their *clv* single mutant counterparts (Fig. 1), a surprising result given that *sqn* mutants have more extra organs than the wild type, not less. To determine the proportional importance of miR172-dependent and independent mechanisms in the meristem phenotypes of *sqn* mutants would require the examination of a plant that is mutant for SQN and all six miR172 targets simultaneously.

In conclusion, SQN contributes to both stem cell homeostasis and floral stem cell termination. Although other targets of miR172, as well as other miRNAs, might also be involved, the influence of SQN on stem cell dynamics appears to be largely mediated by the miR172/*AP2* tandem, which in turn modulates CLV signalling, and *AG* expression. Modulation of CLV signalling seems sufficient to explain the effect of SQN on stem cell homeostasis, but not on floral determinacy. SQN promotes stem cell termination in the flower by activating the expression of *AG* in the centre of the flower (Prunet *et al.*,

2008). This activation of *AG* probably depends on both the CLV pathway, which has a positive effect on *AG* transcription in this domain (Clark *et al.*, 1993), and the down-regulation of AP2, which is a direct repressor of *AG* (Drews *et al.*, 1991; Jofuku *et al.*, 1994; Yant *et al.*, 2010). Overall, the present data shed new light on several important factors that contribute to the robustness of stem cell dynamics in *Arabidopsis*.

Supplementary data

Supplementary data are available at *JXB* online.

Figure S1. *SQN* mRNA level in wild-type and *sqn* mutant plants.

Figure S2. *sqn-4* and *clv3-2* siliques with extra carpels developing above the base of the gynoecium

Figure S3. *sqn-4* inflorescence meristem branching after fasciation.

Figure S4. *sqn-4* mutants exhibit an enlarged central zone.

Figure S5. Peduncles of senesced *SQN 35S::CLV3* and *sqn-4 35S::CLV3* flowers.

Table S1. *sqn* and *miR172* alleles used in this study

Table S2. Primer list.

Acknowledgements

We thank Claire Lionnet and Ann Lavanway for their help with the microscopy; Meredith Price for her help with *Imaris*; and Xuemei Chen, Jeff Long, and Elliot Meyerowitz for providing seeds and constructs. This work was supported by the Centre National de la Recherche Scientifique, the Institut National de la Recherche Agronomique, the Ecole Normale Supérieure de Lyon, the Université de Lyon, the Institut Universitaire de France, the French Agence Nationale de la Recherche through Grant ANR-05-BLAN-0280-01, and the US National Science Foundation through grant IOS-0926347.

References

- Aukerman MJ, Sakai H. 2003. Regulation of flowering time and floral organ identity by a MicroRNA and its APETALA2-like target genes. *The Plant Cell* **15**, 2730–2741.
- Bechtold N, Pelletier G. 1998. In planta Agrobacterium-mediated transformation of adult *Arabidopsis thaliana* plants by vacuum infiltration. *Methods in Molecular Biology* **82**, 259–266.
- Berardini TZ, Bollman K, Sun H, Poethig RS. 2001. Regulation of vegetative phase change in *Arabidopsis thaliana* by cyclophilin 40. *Science* **291**, 2405–2407.
- Bleckmann A, Simon R. 2009. Interdomain signaling in stem cell maintenance of plant shoot meristems. *Molecules and Cells* **27**, 615–620.
- Brand U, Fletcher JC, Hobe M, Meyerowitz EM, Simon R. 2000. Dependence of stem cell fate in *Arabidopsis* on a feedback loop regulated by CLV3 activity. *Science* **289**, 617–619.
- Carles CC, Lertpiriyapong K, Reville K, Fletcher JC. 2004. The ULTRAPETALA1 gene functions early in *Arabidopsis* development to restrict shoot apical meristem activity and acts through WUSCHEL to regulate floral meristem determinacy. *Genetics* **167**, 1893–1903.
- Chen X. 2004. A microRNA as a translational repressor of APETALA2 in *Arabidopsis* flower development. *Science* **303**, 2022–2025.
- Clark SE, Running MP, Meyerowitz EM. 1993. CLAVATA1, a regulator of meristem and flower development in *Arabidopsis*. *Development* **119**, 397–418.
- Clark SE, Running MP, Meyerowitz EM. 1995. CLAVATA3 is a specific regulator of shoot and floral meristem development affecting the same processes as CLAVATA1. *Development* **121**, 2057–2067.
- Clark SE, Williams RW, Meyerowitz EM. 1997. The CLAVATA1 gene encodes a putative receptor kinase that controls shoot and floral meristem size in *Arabidopsis*. *Cell* **89**, 575–585.
- Dievart A, Dalal M, Tax FE, Lacey AD, Huttly A, Li J, Clark SE. 2003. CLAVATA1 dominant-negative alleles reveal functional overlap between multiple receptor kinases that regulate meristem and organ development. *The Plant Cell* **15**, 1198–1211.
- Drews GN, Bowman JL, Meyerowitz EM. 1991. Negative regulation of the *Arabidopsis* homeotic gene AGAMOUS by the APETALA2 product. *Cell* **65**, 991–1002.
- Earley KW, Poethig RS. 2011. Binding of the cyclophilin 40 ortholog SQUINT to Hsp90 protein is required for SQUINT function in *Arabidopsis*. *Journal of Biological Chemistry* **286**, 38184–38189.
- Earley K, Smith M, Weber R, Gregory B, Poethig R. 2010. An endogenous F-box protein regulates ARGONAUTE1 in *Arabidopsis thaliana*. *Silence* **1**, 15.
- Fletcher JC. 2001. The ULTRAPETALA gene controls shoot and floral meristem size in *Arabidopsis*. *Development* **128**, 1323–1333.
- Fletcher JC, Brand U, Running MP, Simon R, Meyerowitz EM. 1999. Signaling of cell fate decisions by CLAVATA3 in *Arabidopsis* shoot meristems. *Science* **283**, 1911–1914.
- Iki T, Yoshikawa M, Nishikiori M, Jaudal MC, Matsumoto-Yokoyama E, Mitsuhashi I, Meshi T, Ishikawa M. 2010. *In vitro* assembly of plant RNA-induced silencing complexes facilitated by molecular chaperone HSP90. *Molecular Cell* **39**, 282–291.
- Ishiguro S, Watanabe Y, Ito N, Nonaka H, Takeda N, Sakai T, Kanaya H, Okada K. 2002. SHEPHERD is the *Arabidopsis* GRP94 responsible for the formation of functional CLAVATA proteins. *EMBO Journal* **21**, 898–908.
- Ito T. 2011. Coordination of flower development by homeotic master regulators. *Current Opinion in Plant Biology* **14**, 53–59.
- Jeong S, Trotochaud AE, Clark SE. 1999. The *Arabidopsis* CLAVATA2 gene encodes a receptor-like protein required for the stability of the CLAVATA1 receptor-like kinase. *The Plant Cell* **11**, 1925–1934.
- Ji L, Liu X, Yan J, *et al.* 2011. ARGONAUTE10 and ARGONAUTE1 regulate the termination of floral stem cells through two microRNAs in *Arabidopsis*. *PLoS Genetics* **7**, e1001358.
- Jofuku KD, den Boer BG, Van Montagu M, Okamoto JK. 1994. Control of *Arabidopsis* flower and seed development by the homeotic gene APETALA2. *The Plant Cell* **6**, 1211–1225.
- Karimi M, Inze D, Depicker A. 2002. GATEWAY vectors for Agrobacterium-mediated plant transformation. *Trends in Plant Science* **7**, 193–195.
- Kayes JM, Clark SE. 1998. CLAVATA2, a regulator of meristem and organ development in *Arabidopsis*. *Development* **125**, 3843–3851.
- Kinoshita A, Betsuyaku S, Osakabe Y, Mizuno S, Nagawa S, Stahl Y, Simon R, Yamaguchi-Shinozaki K, Fukuda H, Sawa S. 2010. RPK2 is an essential receptor-like kinase that transmits the CLV3 signal in *Arabidopsis*. *Development* **137**, 3911–3920.
- Kondo T, Sawa S, Kinoshita A, Mizuno S, Kakimoto T, Fukuda H, Sakagami Y. 2006. A plant peptide encoded by CLV3 identified by *in situ* MALDI-TOF MS analysis. *Science* **313**, 845–848.
- Laux T, Mayer KF, Berger J, Jurgens G. 1996. The WUSCHEL gene is required for shoot and floral meristem integrity in *Arabidopsis*. *Development* **122**, 87–96.
- Lenhard M, Bohnert A, Jurgens G, Laux T. 2001. Termination of stem cell maintenance in *Arabidopsis* floral meristems by interactions between WUSCHEL and AGAMOUS. *Cell* **105**, 805–814.
- Lenhard M, Laux T. 2003. Stem cell homeostasis in the *Arabidopsis* shoot meristem is regulated by intercellular movement of CLAVATA3 and its sequestration by CLAVATA1. *Development* **130**, 3163–3173.
- Liu X, Kim YJ, Muller R, Yumul RE, Liu C, Pan Y, Cao X, Goodrich J, Chen X. 2011. AGAMOUS terminates floral stem cell maintenance in *Arabidopsis* by directly repressing WUSCHEL through recruitment of Polycomb Group proteins. *The Plant Cell* **23**, 3654–3670.
- Lohmann JU, Hong RL, Hobe M, Busch MA, Parcy F, Simon R, Weigel D. 2001. A molecular link between stem cell regulation and floral patterning in *Arabidopsis*. *Cell* **105**, 793–803.
- Mandel T, Moreau F, Kutsher Y, Fletcher JC, Carles CC, Eshed Williams L. 2014. The ERECTA receptor kinase regulates *Arabidopsis* shoot apical meristem size, phyllotaxy and floral meristem identity. *Development* **141**, 830–841.
- Mayer KF, Schoof H, Haecker A, Lenhard M, Jurgens G, Laux T. 1998. Role of WUSCHEL in regulating stem cell fate in the *Arabidopsis* shoot meristem. *Cell* **95**, 805–815.

- Muller R, Bleckmann A, Simon R.** 2008. The receptor kinase CORYNE of Arabidopsis transmits the stem cell-limiting signal CLAVATA3 independently of CLAVATA1. *The Plant Cell* **20**, 934–946.
- Ogawa M, Shinohara H, Sakagami Y, Matsubayashi Y.** 2008. Arabidopsis CLV3 peptide directly binds CLV1 ectodomain. *Science* **319**, 294.
- Ohyama K, Shinohara H, Ogawa-Ohnishi M, Matsubayashi Y.** 2009. A glycopeptide regulating stem cell fate in Arabidopsis thaliana. *Nature Chemical Biology* **5**, 578–580.
- Park W, Li J, Song R, Messing J, Chen X.** 2002. CARPEL FACTORY, a Dicer homolog, and HEN1, a novel protein, act in microRNA metabolism in Arabidopsis thaliana. *Current Biology* **12**, 1484–1495.
- Prigge MJ, Otsuga D, Alonso JM, Ecker JR, Drews GN, Clark SE.** 2005. Class III homeodomain-leucine zipper gene family members have overlapping, antagonistic, and distinct roles in Arabidopsis development. *The Plant Cell* **17**, 61–76.
- Prunet N, Morel P, Negrutiu I, Trehin C.** 2009. Time to stop: flower meristem termination. *Plant Physiology* **150**, 1764–1772.
- Prunet N, Morel P, Thierry AM, Eshed Y, Bowman JL, Negrutiu I, Trehin C.** 2008. REBELOTE, SQUINT, and ULTRAPETALA1 function redundantly in the temporal regulation of floral meristem termination in Arabidopsis thaliana. *The Plant Cell* **20**, 901–919.
- Reddy GV, Meyerowitz EM.** 2005. Stem-cell homeostasis and growth dynamics can be uncoupled in the Arabidopsis shoot apex. *Science* **310**, 663–667.
- Rojo E, Sharma VK, Kovaleva V, Raikhel NV, Fletcher JC.** 2002. CLV3 is localized to the extracellular space, where it activates the Arabidopsis CLAVATA stem cell signaling pathway. *The Plant Cell* **14**, 969–977.
- Schmid M, Uhlenhaut NH, Godard F, Demar M, Bressan R, Weigel D, Lohmann JU.** 2003. Dissection of floral induction pathways using global expression analysis. *Development* **130**, 6001–6012.
- Schoof H, Lenhard M, Haecker A, Mayer KF, Jurgens G, Laux T.** 2000. The stem cell population of Arabidopsis shoot meristems is maintained by a regulatory loop between the CLAVATA and WUSCHEL genes. *Cell* **100**, 635–644.
- Smith MR, Willmann MR, Wu G, Berardini TZ, Moller B, Weijers D, Poethig RS.** 2009. Cyclophilin 40 is required for microRNA activity in Arabidopsis. *Proceedings of the National Academy of Sciences, USA* **106**, 5424–5429.
- Smyth DR, Bowman JL, Meyerowitz EM.** 1990. Early flower development in Arabidopsis. *The Plant Cell* **2**, 755–767.
- Sun B, Xu Y, Ng KH, Ito T.** 2009. A timing mechanism for stem cell maintenance and differentiation in the Arabidopsis floral meristem. *Genes and Development* **23**, 1791–1804.
- Williams L, Grigg SP, Xie M, Christensen S, Fletcher JC.** 2005. Regulation of Arabidopsis shoot apical meristem and lateral organ formation by microRNA miR166g and its AtHD-ZIP target genes. *Development* **132**, 3657–3668.
- Wurschum T, Gross-Hardt R, Laux T.** 2006. APETALA2 regulates the stem cell niche in the Arabidopsis shoot meristem. *The Plant Cell* **18**, 295–307.
- Yadav RK, Perales M, Gruel J, Girke T, Jonsson H, Reddy GV.** 2011. WUSCHEL protein movement mediates stem cell homeostasis in the Arabidopsis shoot apex. *Genes and Development* **25**, 2025–2030.
- Yant L, Mathieu J, Dinh TT, Ott F, Lanz C, Wollmann H, Chen X, Schmid M.** 2010. Orchestration of the floral transition and floral development in Arabidopsis by the bifunctional transcription factor APETALA2. *The Plant Cell* **22**, 2156–2170.
- Yumul RE, Kim YJ, Liu X, Wang R, Ding J, Xiao L, Chen X.** 2013. POWERDRESS and diversified expression of the MIR172 gene family bolster the floral stem cell network. *PLoS Genetics* **9**, e1003218.
- Zhao L, Kim Y, Dinh TT, Chen X.** 2007. miR172 regulates stem cell fate and defines the inner boundary of APETALA3 and PISTILLATA expression domain in Arabidopsis floral meristems. *The Plant Journal* **51**, 840–849.